iScience

CellPress
OPEN ACCESS

Article

Self-regulation of MGAT4A and MGAT4B activity toward glycoproteins through interaction of lectin domain with their own *N*-glycans

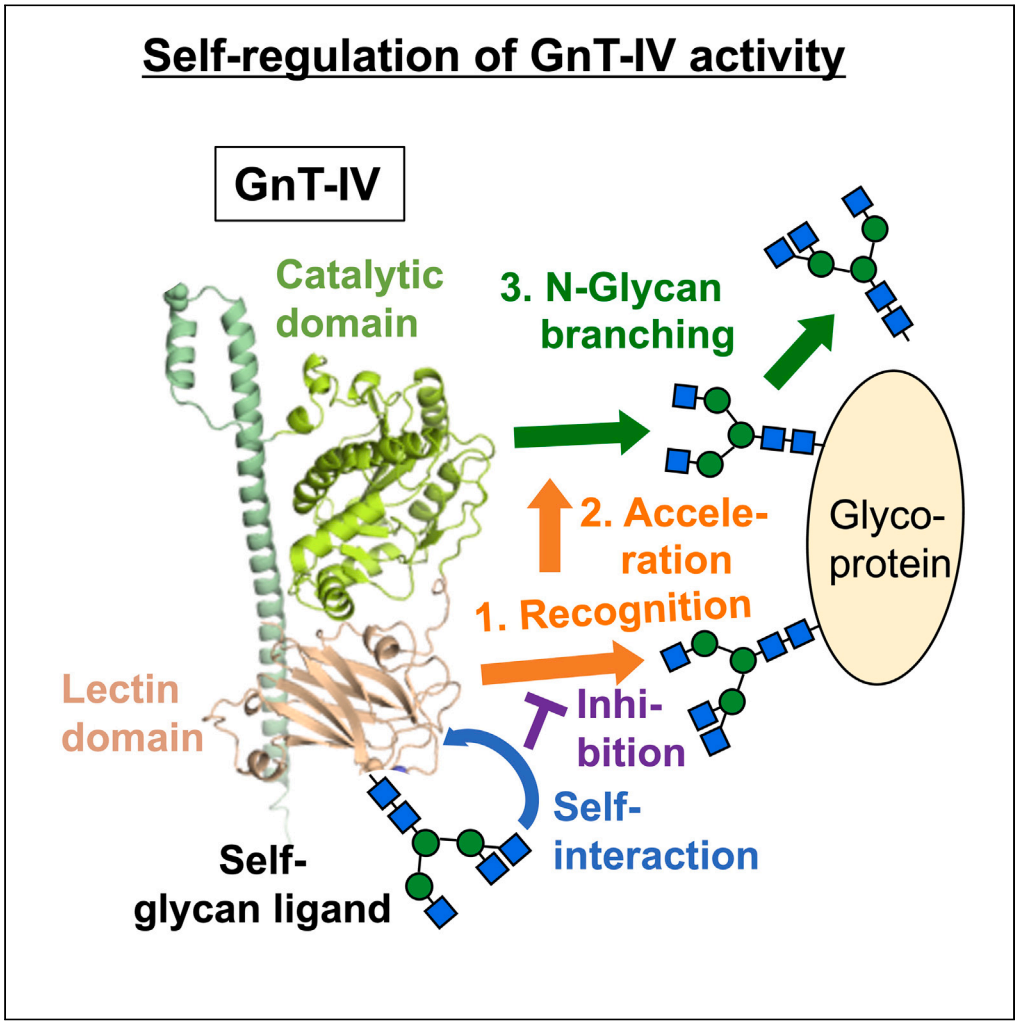

Naoko Osada, Sushil K. Mishra, Miyako Nakano, Yuko Tokoro, Masamichi Nagae, Robert J. Doerksen, Yasuhiko Kizuka

kizuka.yasuhiko.k8@f.gifu-u.ac.jp

Highlights

GnT-IVa and -IVb are GlcNAc transferases having a C-terminal lectin domain

Lectin domain is pivotal for activity toward glycoproteins but not free glycans

Lectin domain has an *N*-glycan which likely inhibits ligand binding

Activity of GnT-IVa and -IVb is self-regulated by their own *N*-glycans

Osada et al., iScience *27*, 111066
November 15, 2024
https://doi.org/10.1016/j.isci.2024.111066

iScience

CellPress
OPEN ACCESS

Article

Self-regulation of MGAT4A and MGAT4B activity toward glycoproteins through interaction of lectin domain with their own *N*-glycans

Naoko Osada,[1] Sushil K. Mishra,[2] Miyako Nakano,[3] Yuko Tokoro,[4] Masamichi Nagae,[5,6] Robert J. Doerksen,[2] and Yasuhiko Kizuka[1,4,7,*]

SUMMARY

***N*-Acetylglucosaminyltransferases-IVa (GnT-IVa or MGAT4A) and -IVb (MGAT4B) are glycosyltransferase isozymes synthesizing the β1,4-GlcNAc branch in *N*-glycans, a glycan structure involved in diabetes. These enzymes uniquely have a non-catalytic lectin domain, which selectively recognizes the GnT-IV product *N*-glycan branch, but the role of this lectin domain has remained unclear. Here, using UDP-Glo enzyme assays, we discovered that this domain is required for activity toward glycoprotein substrates but not toward free glycans. Furthermore, we found that the lectin domain itself is decorated with an *N*-glycan, which can serve as a self-ligand and interact with the ligand binding site of the lectin domain in a glycan structure-dependent manner. Enzyme assays using glycan-remodeled GnT-IVa demonstrated that the interaction of the self-ligand with the lectin domain suppresses GnT-IVa activity toward glycoprotein substrates. These findings unveiled a lectin-assisted self-regulatory mechanism of glycosyltransferases, which deepens our understanding of the complex pathway of *N*-glycan biosynthesis.**

INTRODUCTION

Glycosylation, one of the most common post-translational modifications in mammals, has many key biological roles such as in regulation of protein stability, signal transduction, and intercellular adhesion.[1] It has been estimated that more than 50% of the proteins in eukaryotes are glycosylated,[2] and structurally diverse glycans contribute to the regulation of myriad biological phenomena, including immune surveillance, inflammatory reactions, neural activity and plasticity, hormone signaling, and tumor metastasis.[3] Therefore, abnormalities in glycosylation are involved in a wide variety of human diseases, such as cancer,[4] diabetes,[5] and Alzheimer's disease.[6] Understanding how protein glycosylation is regulated and how it becomes abnormal in cells may help to elucidate pathogenic mechanisms and develop new diagnostics and therapies against glycan-related diseases.

N-Glycans, on which we focus in this paper, have complex biosynthetic mechanisms.[7] In eukaryotes, the Asn residue in the consensus sequence, Asn-X-Ser/Thr, in which "X" is any amino acid except Pro,[7] first receives transfer of the assembled oligosaccharide from the lipid (dolicholpyrophosphate)-linked glycan donor in the ER lumen.[8] After trimming of the terminal Glc and Man residues, core fucosylation and GlcNAc branching are catalyzed in the Golgi apparatus by sequential actions of glycosyltransferases,[9] followed by further elongation of *N*-glycans with tremendous structural complexity. The GlcNAc branches of *N*-glycans are biosynthesized by *N*-acetylglucosaminyltransferases-I–V (GnT-I–V, also designated as MGAT1–5) in protein- and glycosylation site-selective manners.[10] The expression levels of these branching enzymes and their product glycans are altered, under various pathophysiological conditions,[11] and these are in turn involved in the onset and aggravation of various diseases. However, the detailed mechanisms of activity regulation and specificity of GnTs in cells remain largely unclear. In particular, how target proteins are selectively modified by each GnT in cells remains to be clarified.

Among these branching enzymes, GnT-IV has unique structures, functions, and homologs. The GnT-IV family has four homologous members in humans: GnT-IVa (MGAT4A), GnT-IVb (MGAT4B), GnT-IVc (MGAT4C, also known as GnT-VI), and GnT-IVd (MGAT4D, also known as GnT-1IP).[12–14] Among these four members, only GnT-IVa and GnT-IVb isoenzymes have GnT-IV activity to transfer GlcNAc from UDP-GlcNAc to the α1,3-Man arm of an *N*-glycan via a β1,4-linkage (Figure 1A). As to the functions of this branch, GnT-IVa-deficient mice showed reduced cell surface residency of GLUT2 in pancreatic beta cells, resulting in impaired glucose-stimulated insulin secretion and a type-2 diabetic

[1]Graduate School of Natural Science and Technology, Gifu University, Gifu 501-1193, Japan
[2]Glycoscience Center of Research Excellence, Department of BioMolecular Sciences, University of Mississippi, Oxford, MS 38677, USA
[3]Graduate School of Integrated Sciences for Life, Hiroshima University, Higashihiroshima 739-8530, Japan
[4]Institute for Glyco-core Research (iGCORE), Gifu University, Gifu 501-1193, Japan
[5]Department of Molecular Immunology, Research Institute for Microbial Diseases, Osaka University, Suita 565-0871, Japan
[6]Laboratory of Molecular Immunology, Immunology Frontier Research Center (IFReC), Osaka University, Suita 565-0871, Japan
[7]Lead contact
*Correspondence: kizuka.yasuhiko.k8@f.gifu-u.ac.jp
https://doi.org/10.1016/j.isci.2024.111066

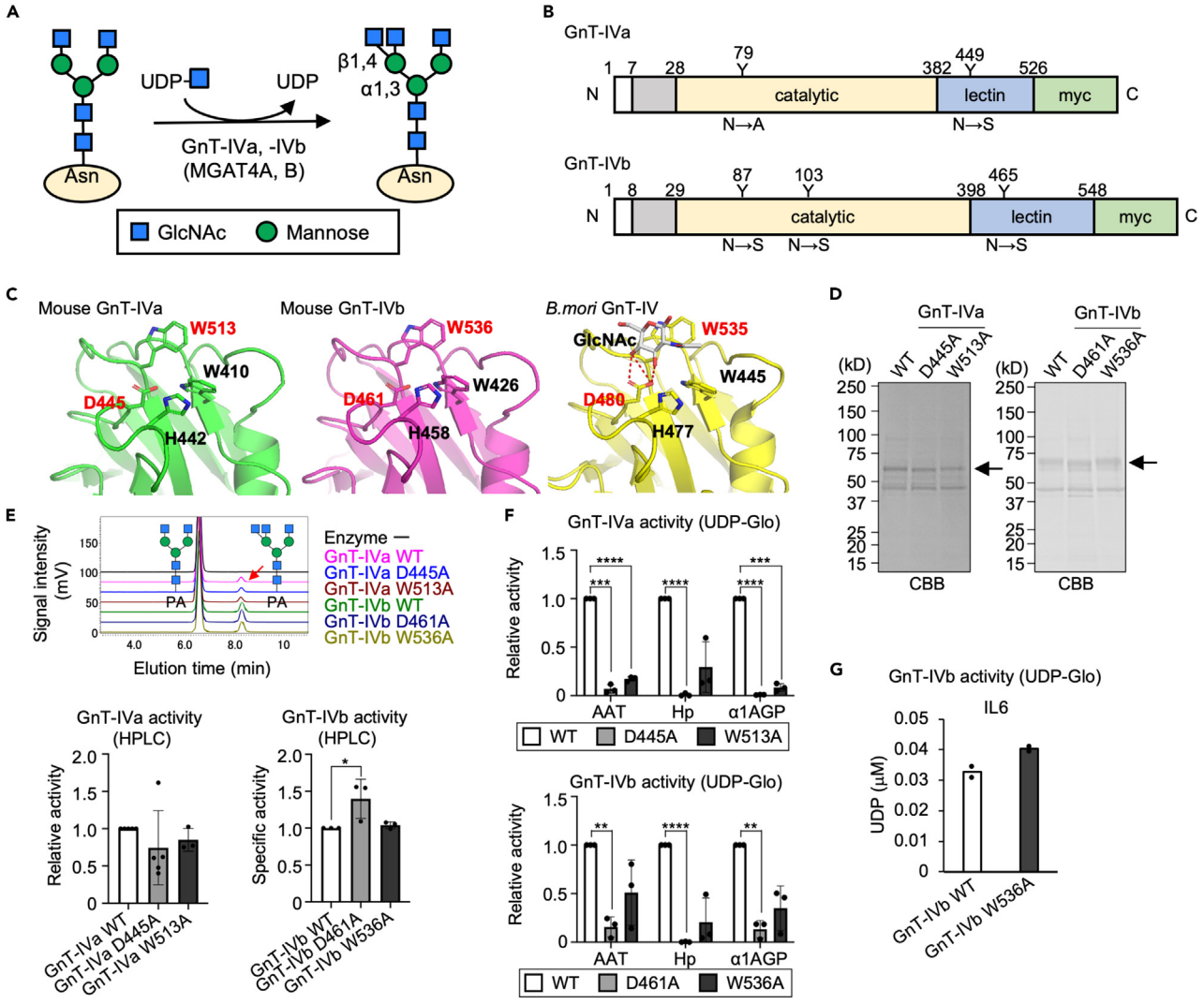

Figure 1. Activity of lectin domain mutants of GnT-IVa and -IVb

(A) Schematic model of the GlcNAc transfer reaction catalyzed by GnT-IVa and -IVb (MGAT4A and MGAT4B).

(B) Domain structures and *N*-glycosylation sites of mouse GnT-IVa and -IVb constructs used for this study.

(C) The structures of GlcNAc binding sites of the lectin domains of GnT-IVa (green, PDB ID: 7VMT), GnT-IVb (magenta, AlphaFold2), and *B. mori* GnT-IV (yellow, PDB ID: 7XTN). Residues critical to ligand binding (D445 and W513 in GnT-IVa, D461 and W536 in GnT-IVb, and D480 and W535 in silkworm GnT-IV) are shown in red.

(D) Soluble GnT-IVa and -IVb, and their mutants were expressed in COS7 cells and purified from the medium using a Ni^{2+} column. Purified GnT-IV enzymes were separated by SDS-PAGE and visualized by CBB staining.

(E) Activity of purified GnT-IV was measured by incubating the enzymes with GnGnbi-PA and performing analysis using HPLC. The specific activity was calculated from the peak area (n = 3–5, mean ± SD, *$p < 0.05$, Tukey's multiple comparisons test).

(F) Comparison of the *in vitro* activity of purified soluble GnT-IV WT and lectin domain mutants toward various glycoproteins. The activity was measured using UDP-Glo assay ($n = 3$, mean ± SD, **$p < 0.01$, ***$p < 0.001$, ****$p < 0.0001$, Tukey's multiple comparisons test).

(G) Comparison of the *in vitro* activity of purified soluble GnT-IVb WT and W536A mutant toward singly glycosylated IL6. The activity was measured using UDP-Glo assay ($n = 2$, means and each data points are shown).

phenotype.[5] Downregulation of GnT-IVa gene expression was also found in diabetic human beta cells.[15] These findings demonstrate that GnT-IVa plays crucial roles in glucose metabolism by modifying the functions of the particular proteins that serve selectively as its substrates.

Similar to many other Golgi glycosyltransferases, GnT-IV enzymes have a type-II transmembrane topology, consisting of a short cytoplasmic tail, a membrane-spanning domain, a stem region, and a large luminal region with a few *N*-glycosylation sites (Figure 1B).[16] Intriguingly, we recently found a unique lectin domain in the C-terminal region of GnT-IVa unlike other *N*-glycan biosynthetic enzymes, solved its crystal structure, and analyzed its glycan binding specificity.[17] This lectin domain is conserved among GnT-IVa, GnT-IVb, and GnT-IVc, and

our analysis of the GnT-IVa lectin domain revealed that it preferentially recognizes the product glycans of the GnT-IVa reaction with GlcNAc termini.[17] In addition, a deletion mutant of GnT-IVa lacking the lectin domain was found to be completely unfunctional.[17] These findings strongly suggest that GnT-IVa and GnT-IVb have GlcNAc-branching mechanisms in cells involving their lectin domains, but the detailed roles of the lectin domain are not understood.

Regarding the functions of the GnT-IV lectin domain, we have recently shown that a point mutant swapping a residue in the lectin domain between GnT-IVa and GnT-IVb altered its preference of glycoprotein substrates.[18] Furthermore, we showed that GnT-IVa and GnT-IVb have different preference for substrate proteins, and GnT-IVb particularly prefers glycoproteins which were partially pre-modified by GnT-IVa or GnT-IVb. These findings raised the possibility that the lectin domains of GnT-IVa and GnT-IVb are involved in recognition of glycoprotein substrates through binding to their *N*-glycans.

In this study, we investigated the function of the lectin domain. Using biochemical and structural approaches, we revealed that the lectin domain is required for activity toward glycoprotein substrates but not toward free glycan substrates. We also showed that such lectin-assisted glycosylation of proteins by GnT-IVa and GnT-IVb is regulated by their own *N*-glycans, highlighting a unique self-regulatory mechanism of glycosyltransferases.

RESULTS

Lectin domains of GnT-IVa and -IVb are essential for enzymatic activity toward glycoprotein substrates

To clarify how its lectin domain regulates GnT-IV activity, we first established GnT-IV point mutants lacking only lectin activity. On the basis of the crystal structure of the lectin domains of mouse GnT-IVa apo-form[17] and *B. mori* GnT-IV in complex with GlcNAc,[19] we found that the structure of the GlcNAc binding site in the GnT-IV lectin domain is conserved among GnT-IVa and GnT-IVb isozymes and among various species (Figure 1C). In particular, an Asp and a Trp (D445 and W513 in mouse GnT-IVa, D461 and W536 in mouse GnT-IVb) are probably critical for the interaction with glycan ligands (Figure 1C). Consistent with this, the D445A mutation in the mouse GnT-IVa lectin domain was previously shown to lead to the loss of glycan binding ability,[17] demonstrating the importance of that residue for glycan binding.

To examine whether the glycan binding ability of the lectin domain is required for the enzyme activity, recombinant soluble GnT-IVa and -IVb WT and mutants in which either one of the two key residues in the lectin domains were mutated were expressed in COS7 cells and purified from the culture media (Figure 1D). The *in vitro* activity of these mutants toward a free glycan and glycoproteins was measured (Figures 1E and 1F). For the activity toward the glycan, a fluorescence-labeled GlcNAc-terminated biantennary *N*-glycan (GnGnbi-PA) was used as a substrate,[20] and the reaction mixtures were analyzed by reverse-phase HPLC (Figure 1E, upper). Although GnT-IVa D445A showed a tendency of weaker activity than WT,[17] the activity toward the free glycan substrate was basically retained in the lectin domain mutants for both GnT-IVa and GnT-IVb (Figure 1E, lower), suggesting that the lectin domain has functions other than to affect the sugar transfer reaction itself. Because we previously found that the lectin domain affects selectivity toward glycoprotein substrates,[18] we hypothesized that the lectin domain plays key roles in the recognition of glycoprotein substrates. To test this hypothesis, the activity toward glycoprotein substrates was measured for the lectin domain mutants using the UDP-Glo assay (Figure 1F). In this assay, the level of UDP released from UDP-GlcNAc by a glycosyltransferase reaction is measured,[21] and we recently implemented GnT activity assays for various acceptor glycoproteins.[18,21,22] Using this assay system, we measured the activity of GnT-IV WT and the lectin domain mutants toward three human plasma glycoproteins, alpha-1-antitrypsin (AAT), haptoglobin (Hp), and alpha-1-acid glycoprotein (α1AGP), which have multiple *N*-glycosylation sites (AAT: 3; Hp: 4; α1AGP: 5). Surprisingly, the lectin domain mutants showed dramatically reduced activity toward all glycoprotein substrates for both GnT-IVa and GnT-IVb (Figure 1F). This demonstrates that the GnT-IV lectin domains are essential for the enzyme activity toward glycoprotein substrates, while it is basically dispensable for the sugar transfer reaction itself toward an acceptor glycan.

Since the above glycoprotein substrates (AAT, Hp and α1AGP) all have multiple glycans, we next tested a glycoprotein substrate which has only one *N*-glycan. Human Interleukin 6 (IL-6) has two potential glycosylation sites, but only the first site (N73) is known to be *N*-glycosylated.[23] Recombinant IL-6 produced from HEK293 cells was first treated with neuraminidase and β-galactosidase so that its glycan structure was made to be suitable as a substrate for GnT-IVs (Figure S1). The UDP-Glo assay results showed that the activity of the GnT-IVb W536A mutant toward IL-6 was not lower but even higher than WT (Figure 1G). This suggests that the lectin domain of GnT-IVb recognizes glycoprotein substrates bearing multi-*N*-glycans for efficient reaction.

Interaction between GnT-IV's own N-glycan and glycan binding site of lectin domain

GnT-IVa and b are both *N*-glycosylated (Figures 1B and 2A), and we noticed that one *N*-glycan attached to the lectin domain is proximate to the ligand binding site (Figure 2B). We thus hypothesized that the *N*-glycan on the lectin domain interacts with the glycan binding site as a self-ligand, thereby regulating GnT-IVa and -IVb activity. To test this possibility, we first confirmed that GnT-IVa and GnT-IVb are indeed *N*-glycosylated, as shown by a band shift upon *N*-glycan removal with PNGaseF (Figure 2C, left). The lower band of GnT-IVb is PNGaseF-resistant, suggesting that GnT-IVb exists as both glycosylated and non-glycosylated forms when expressed in the cells. In addition, point mutation at the consensus sequon in the lectin domain (N449 for GnT-IVa and N465 for GnT-IVb) as well as mutation at the other sites resulted in a down-shift in SDS-PAGE (Figure 2C, right), indicating that the lectin domain itself is *N*-glycosylated. Furthermore, the *N*-glycosylation site and the glycan binding site of the lectin domain are highly conserved in a variety of species (Figure 2D), suggesting that the *N*-glycan near the glycan binding site plays some important roles in regulation of the lectin domain.

To examine whether GnT-IV's own *N*-glycan can bind to the lectin domain, extensive molecular dynamics (MD) simulations of the lectin domain with different *N*-glycan structures were performed (Figures 2E–2L, S2, and S3). The ring conformation for each monosaccharide

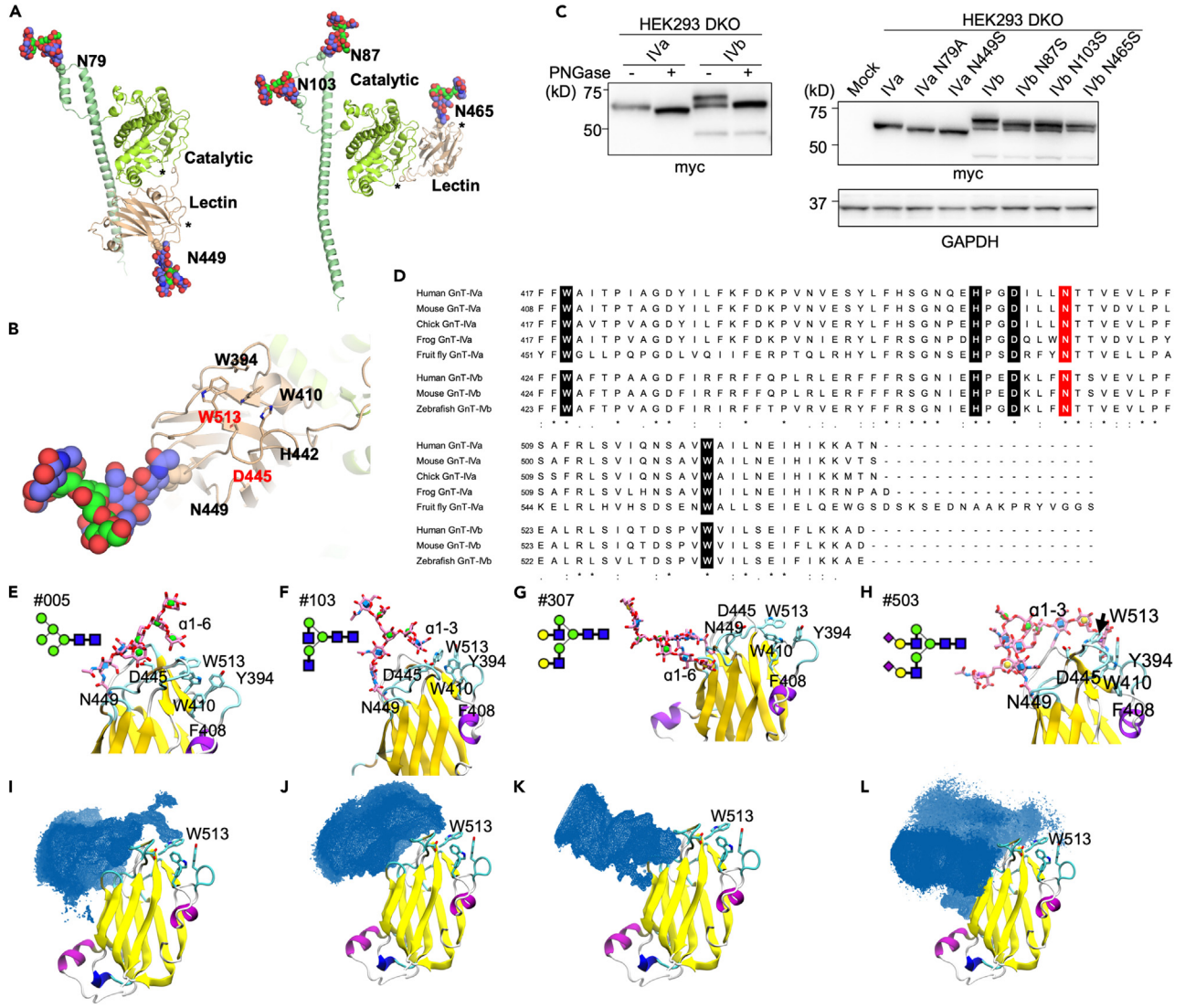

Figure 2. Possible interaction of GnT-IV's own *N*-glycan with the lectin domain

(A) Structure models of glycosylated GnT-IVa and -IVb. *N*-Glycans are shown as ball models.

(B) Close-up view of the glycan binding site and the self *N*-glycan in the GnT-IVa lectin domain.

(C) Proteins from HEK293 GnT-IVa and -IVb DKO cells transfected with a plasmid for the expression of GnT-IVa or GnT-IVb were treated with PNGaseF and blotted with anti-myc antibody (*left*). Proteins from HEK293 DKO cells transfected with an empty vector (mock) or a plasmid for expression of GnT-IVa or GnT-IVb and their *N*-glycosylation site mutants were subjected to SDS-PAGE and blotted with anti-myc antibody (*upper right*) and anti-GAPDH antibody (*lower right*).

(D) Sequence comparison of the lectin domains of GnT-IVa and -IVb in various species (human, mouse, chicken, frog, fruit fly, and zebrafish). Glycan binding site (black) and *N*-glycosylation site (red) are highlighted.

(E–L) MD simulation of interaction of GnT-IVa lectin domain with its own *N*-glycan. Selected conformations from MD simulations are shown: oligomannose (E), agalactosylated (F), galactosylated (G), and sialylated (H) *N*-glycans. The corresponding *N*-glycan grid maps, depicting conformational space with blue dots, are in the bottom row (I–L).

and the dihedral angles of all glycosidic linkages were calculated and analyzed (Figures S4–S6 and Table S1). The GnT-IVa lectin domain is capable of binding to GlcNAc via polar interactions with D445 and CH–π stacking interactions with W513 (Figure S2A). Therefore, we explored whether the *N*-glycan attached to N449 of the lectin domain can flip back and bind to the glycan binding site and affect binding of another ligand to the lectin domain by occupying the GlcNAc binding region.

Among the eight different *N*-glycans tested on N449, the oligomannose *N*-glycan (#005) and agalactosylated *N*-glycans (#103, 105) have the potential to flip back toward the glycan binding site and interact with D445 and W513 (Figures 2E, 2F, 2I, and 2J). In the MD simulations, for the oligomannose *N*-glycan (#005), the Man residue of the α1-6 branch occasionally visited the glycan binding site. The agalactosylated

N-glycans (#103, 105) have a terminal GlcNAc on each branch, and since the lectin domain preferentially binds GlcNAc,[17,19] this type of *N*-glycan has the potential to serve as a self-ligand. In the MD simulations of *N*-glycans #103 and 105, the terminal GlcNAc of the α1-3 branch flipped toward W513 and potentially interacted better with the glycan binding pocket than the oligomannose *N*-glycan (#005). However, such interactions were not steadily maintained once achieved. Rather, the α1-3 branch underwent dynamic change, and several other conformations were observed (Figures S2K and S3). This suggests that a GlcNAc-terminated *N*-glycan can serve as a self-ligand while its interactions with the ligand binding site are transient and dynamic.

In contrast, the galactosylated *N*-glycans (#307, 313) showed a very different but consistent behavior, in which the α1-3 branch bound to a loop containing D445 and the GlcNAc of the α1-6 branch made stacking interactions with Y485. These terminal Gal-containing *N*-glycans do not interact with W513 and are thus highly unlikely to serve as self-ligands (Figures 2G–2K, S2E, S2F, S3D, and S3E). The sialylated *N*-glycans (#503, 504, 506) have long and bulky branches that are long enough to reach the glycan binding site (Figures 2H, 2L, S2H–S2J), but they also did not exhibit any stable interaction with W513. Rather, they demonstrated dynamic behavior and adopted multiple conformations in and around the glycan binding site, especially for #504 and 506 (Figure S2K). Furthermore, the full-length structures of the GnT-IVa homodimer and the heterodimer of GnT-IVa with GnT-IVb, predicted by AlphaFold Multimer, reveal that N449 of one monomer is significantly distant from the Trp residue in the ligand binding site of the other monomer (W513 in GnT-IVa and W536 in GnT-IVb) (Figure S7). This suggests that the *N*-glycan from one monomer cannot bind to the glycan binding site of the other monomer.

Overall, the MD simulations strongly suggest that agalactosylated *N*-glycans have the potential to bind to the glycan binding site of GnT-IVa lectin domain better than oligomannose *N*-glycans. The sialylated *N*-glycans can also potentially affect the glycan binding by visiting the binding site region for short times and by occupying neighboring space required for substrate glycoprotein binding, rather than binding directly to W513. By contrast, the galactosylated *N*-glycans are unlikely to interfere with glycan binding to the lectin domain.

The structures of GnT-IV's own N-glycans contain self-ligands for the lectin domain

The MD simulation results suggested that the interactions between the lectin domain and a self-ligand depend on the type of *N*-glycan that is attached. We therefore investigated whether the self-ligand attachment site (N449 of GnT-IVa or N465 of GnT-IVb) is modified with strong binders (GlcNAc-terminated glycans) or weak binders (oligomannose and sialylated glycans) in cells. To analyze the site-specific glycan structures of GnT-IV's own *N*-glycans, Myc-tagged full-length GnT-IVa and GnT-IVb were expressed in GnT-IVa,b double-KO (DKO) cells, immunopurified from cell lysates (Figure 3A), and analyzed by LC-MS glycoproteomics (Figures 3B, 3C, and Table S2). We successfully detected *N*-glycopeptides for all potential glycosylation sites (GnT-IVa: N79, N449; GnT-IVb: N87, N103, N465) with various glycan structures (Figures 3B and 3C). We found that the glycan structures, which were mainly composed of oligomannose glycans and GlcNAc-terminated glycans, differ depending on the *N*-glycosylation sites (Figure 3D). Notably, the relative amount of GlcNAc-terminated *N*-glycans was less on the lectin domain (N449 and N465) than on the other sites, for both GnT-IVa and GnT-IVb. These findings show that the *N*-glycan in the lectin domain is modified with self-ligands and occasionally with strong binders.

GnT-IVa activity toward glycoproteins is regulated by the structure of GnT-IVa's own N-glycans

We next examined whether lectin domain-mediated regulation of catalytic activity toward glycoproteins depends on its self-ligand glycan. To this end, we first investigated mutants lacking the *N*-glycosylation site in the lectin domain. However, the GnT-IVa N449S mutant and GnT-IVb N465S mutant showed reduced activity toward glycan substrates (Figure S8A) and reduced Golgi localization (Figure S8B). Furthermore, deletion of the *N*-glycans in soluble truncated enzymes prevented their secretion into the medium (Figure S8C). These findings show that removal of the *N*-glycan in the lectin domain by point mutation resulted in folding defects and that the *N*-glycosylation site mutants are unsuitable for analyzing the functions of the *N*-glycan.

We thus next analyzed the activity of GnT-IVa whose *N*-glycan structures were remodeled. To this end, soluble GnT-IVa was expressed and purified from WT and glyco-engineered cells, and we measured the activity of the purified glycan-remodeled GnT-IVa toward glycoproteins.

We first performed glycoproteomic analysis of soluble truncated GnT-IVa and GnT-IVb purified from HEK293 DKO cells (Figure S9 and Table S3), which revealed that secreted GnT-IVa and GnT-IVb mostly contained galactosylated (non-binder) or sialylated (weak binder) mature *N*-glycans on the lectin domain (Figure S9D), different from full-length GnT-IVa and GnT-IVb in cells. As full-length GnT-IVa and GnT-IVb are mainly decorated with oligomannose (weak binder) and GlcNAc-terminated (strong binder) glycans (Figure 3), we next changed the *N*-glycan structures of GnT-IVa to oligomannose or GlcNAc-terminated glycans.

To obtain GnT-IVa with oligomannose glycans, the soluble form of GnT-IVa was expressed in Expi293 GnT-I KO cells and purified from the culture medium (Figures 4A and S10A). GnT-I is the enzyme responsible for initiating the maturation step of *N*-glycan synthesis,[24] and the glycan structures of GnT-IVa from GnT-I KO cells become exclusively the oligomannose type, particularly Man5. Lectin blotting confirmed that GnT-IVa purified from GnT-I KO cells showed increased reactivity to Man-binding lectin concanavalin A (ConA),[25] and reduced reactivity to GlcNAc-binding lectin *Datura stramonium* agglutinin (DSA)[26] and Gal-binding lectin *Ricinus communis* agglutinin (RCA)[27] (Figures 4B and S10B). Using these GnT-IVa glycoforms, the *in vitro* activity toward a free glycan and glycoproteins was measured (Figures 4C and 4D). The activity of GnT-IVa from GnT-I KO cells toward glycans was reduced compared with that of the enzyme from WT cells, although the reason for this was unknown (Figure 4C). Meanwhile, the activity of the GnT-I KO-derived enzyme toward glycoproteins was comparable to that of the WT-derived enzyme, suggesting that mature *N*-glycans and oligomannose *N*-glycans have similar effects on GnT-IVa and -IVb activity against glycoproteins.

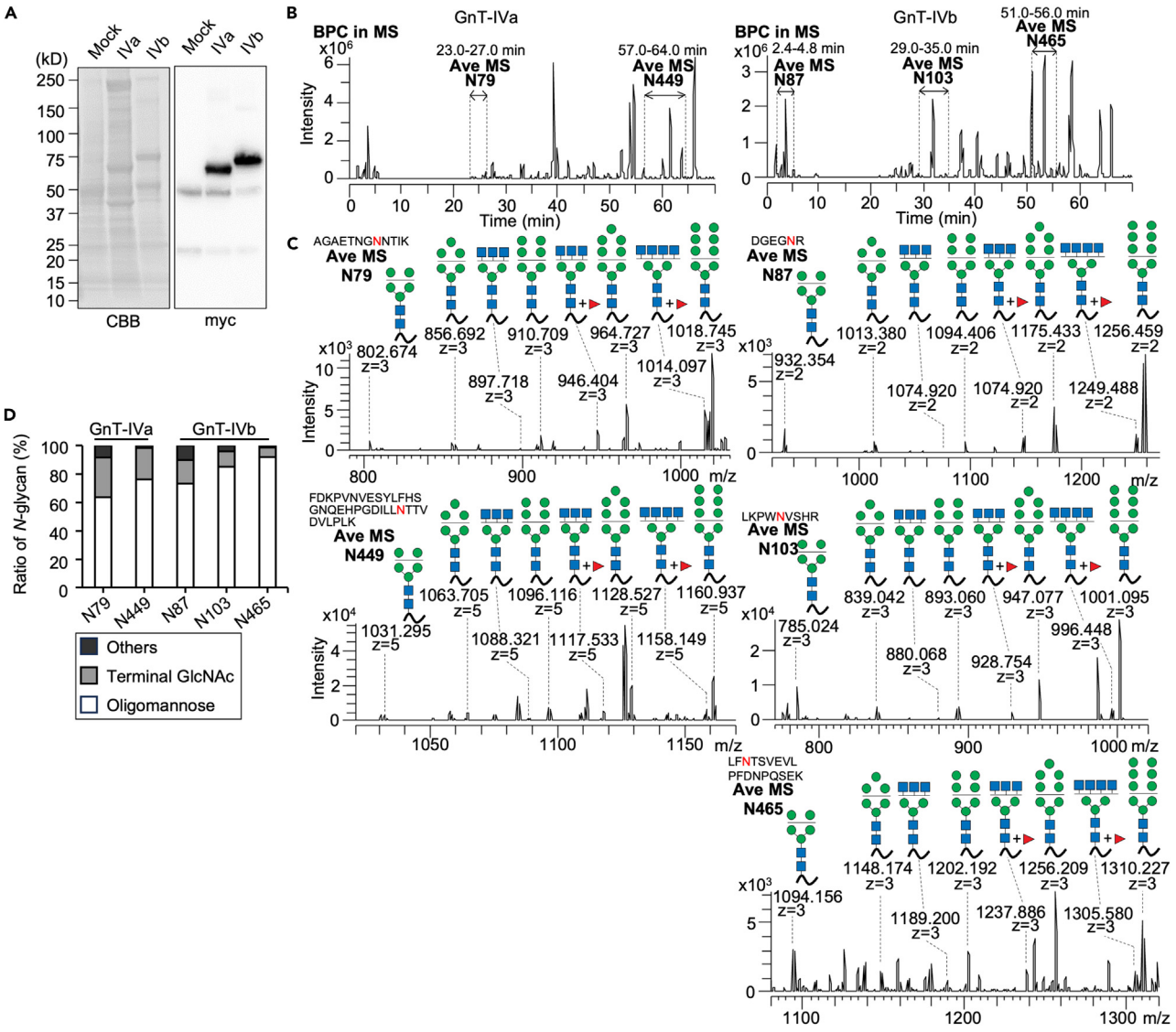

Figure 3. Structural analysis of GnT-IV's own *N*-glycans

(A) Myc-tagged GnT-IVa and GnT-IVb were expressed and immunopurified from DKO lysates. Purified enzymes were subjected to CBB and anti-myc blotting, and subsequently analyzed by LC-MS glycoproteomics.

(B) Base peak chromatogram (BPC) of full-length GnT-IVa- and GnT-IVb-derived peptides digested with trypsin.

(C) Average MS spectrum of a glycopeptide containing N79- or N449-glycan for GnT-IVa and a glycopeptide containing N87-, N103-, or N465-glycan for GnT-IVb. The structures of major N-glycans are shown at the top of the spectrum (All *N*-glycans observed in this analysis are shown in Table S2).

(D) Ratio of oligomannose, GlcNAc-terminated, and other complex-type glycans attached to each site of GnT-IVa and -IVb. Glycans with even one GlcNAc at the end of the glycan were classified as terminal GlcNAc glycans.

Next, to obtain GnT-IVa with GlcNAc-terminated glycans, soluble GnT-IVa was expressed in HEK293 SLC35A2 KO cells that lack the UDP-Gal transporter[28] and purified from the culture medium (Figures 4E and S10C). Lectin blotting confirmed that GnT-IVa purified from SLC35A2 KO cells showed increased reactivity to GlcNAc-binding lectin, DSA and *Griffonia simplicifolia* lectin II (GSLII),[29] and reduced reactivity to RCA (Figures 4F and S10D), demonstrating the expected glycan remodeling of GnT-IVa purified from SLC35A2 KO cells to the higher-affinity ligands for the lectin domain than that from WT cells. Although the activity of GnT-IVa derived from SLC35A2 KO cells toward free glycan was comparable to that of GnT-IVa from WT cells (Figure 4G), the activity of the SLC35A2 KO-derived enzyme toward glycoprotein was significantly reduced compared with that of the WT-derived enzyme (Figure 4H).

Finally, we separated glycoforms of GnT-IVa using lectin-conjugated beads and measured their *in vitro* activity toward glycoproteins. Soluble GnT-IVa was first purified from the HEK293 DKO cell culture media, and GlcNAc-terminated and galactosylated glycoforms were enriched using GSLII- and RCA-beads, respectively. The UDP-Glo results showed that RCA-bound GnT-IVa exhibited higher activity than

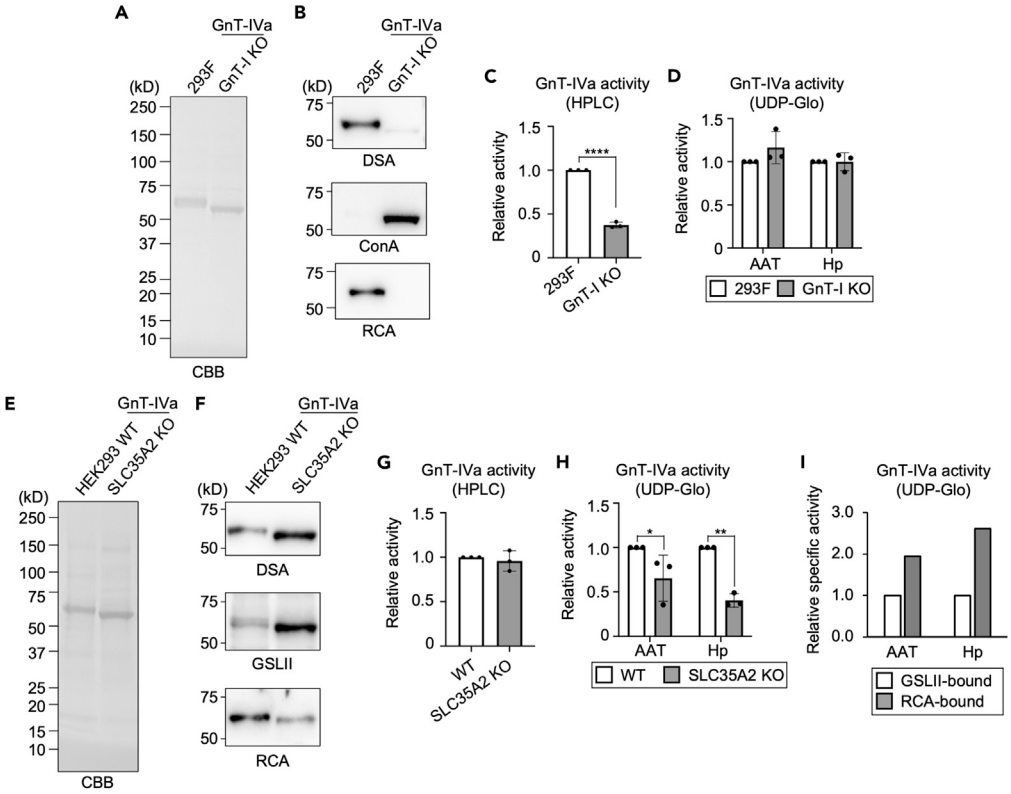

Figure 4. GnT-IV activity toward glycoproteins is regulated by glycan structure

(A) Soluble GnT-IVa was expressed in Expi293F and Expi293 GnT-I KO cells and purified from the medium using a Ni^{2+} column. Purified GnT-IV enzymes were separated by SDS-PAGE and visualized by CBB staining.

(B) Purified GnT-IVa enzymes were subjected to SDS-PAGE and blotted with DSA (*upper*), ConA (*middle*), or RCA (*lower*).

(C) Enzyme activity of purified GnT-IVa was measured by incubating the enzyme with GnGnbi-PA and performing analysis using HPLC. The specific activity was calculated from the peak area ($n = 3$, mean ± SD, ****$p < 0.0001$, unpaired *t* test).

(D) Comparison of the *in vitro* activity of purified soluble GnT-IVa derived from Expi293F and Expi293 GnT-I KO cells toward two glycoproteins. The activity was measured using UDP-Glo assay ($n = 3$, mean ± SD, Holm-Sidak's multiple comparisons test).

(E) Soluble GnT-IVa was expressed in HEK293 WT and HEK293 SLC35A2 KO cells and purified from the medium using a Ni^{2+} column. Purified GnT-IVa enzymes were separated by SDS-PAGE and visualized by CBB staining.

(F) Purified GnT-IV enzymes were subjected to SDS-PAGE and blotted with DSA (*upper*), GSLII (*middle*), or RCA (*lower*).

(G) Enzyme activity of purified GnT-IVa was measured by incubating the enzyme with GnGnbi-PA and performing analysis using HPLC. The specific activity was calculated from the peak area ($n = 3$, mean ± SD, unpaired *t* test).

(H) Comparison of the *in vitro* activity of purified soluble GnT-IVa derived from HEK293 WT and HEK293 SLC35A2 KO cells toward two glycoproteins. The activity was measured using UDP-Glo assay ($n = 3$, mean ± SD, *$p < 0.05$, **$p < 0.01$, Holm-Sidak's multiple comparisons test).

(I) Comparison of the *in vitro* activity of glycoforms of soluble GnT-IVa separated by GSLII- and RCA-conjugated beads. The activity toward two glycoproteins was measured using UDP-Glo assay and divided by the anti-GnT-IVa signal intensity in Figure S10E.

GSLII-bound GnT-IVa (Figures 4I and S10E), further suggesting the suppressive role of GlcNAc-terminated glycan on GnT-IVa for the activity toward glycoproteins. These findings indicate that, if a GnT-IVa glycan is modified with a terminal GlcNAc (conferring higher affinity for the lectin domain), the activity of GnT-IVa is reduced, suggesting that interaction of the self-ligand with the lectin domain negatively regulates GnT-IVa activity toward glycoprotein substrates.

DISCUSSION

In this study, we discovered that the lectin domains are important for GnT-IVa and GnT-IVb activity against glycoprotein substrates. Such lectin-mediated recognition of substrates could be a mechanism for protein-selective synthesis of an *N*-glycan branch, and is specific to GnT-IVs, since no other *N*-glycan biosynthetic enzymes are known to have a lectin domain. Our findings also indicated that the *N*-glycan on the lectin domain may serve as a self-ligand and negatively regulate the lectin-assisted action of GnT-IVa in an *N*-glycan structure-dependent manner (Figure 5). This study demonstrates the self-regulatory mechanism of a glycosyltransferase in which glycosyltransferase activity is regulated by its own specific *N*-glycan.

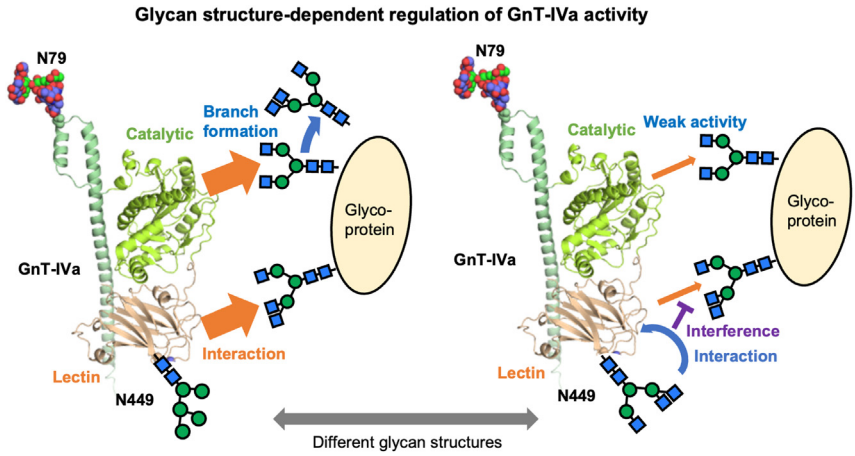

Figure 5. Model of the regulation of function of GnT-IVa lectin domain

(*Left*) The GnT-IVa lectin domain could recognize an *N*-glycan of the glycoprotein substrate, which is required for branch formation by the catalytic domain. A weak binder (e.g., oligomannose glycan) at the *N*-glycosylation site in the lectin domain is unlikely to interfere with the lectin domain's function. (*Right*) A strong binder (e.g., GlcNAc-terminated branched *N*-glycan) works as a self-ligand and interferes with the recognition of glycoprotein substrates by the lectin domain, resulting in negative regulation of catalytic activity.

Our data suggest that the lectin domains of GnT-IVa and -IVb recognize and select glycoprotein substrates. Meanwhile, we previously claimed that the lectin domain is also important for the activity against free glycan substrates, based on the results from one point mutant (D445A) of GnT-IVa.[17] However, the present study using four point mutants (D445A and W513A for GnT-IVa, D461A and W536A for GnT-IVb) showed that the effect of the lectin binding is far higher on glycoprotein substrates (Figure 1F) as opposed to free glycan substrates (Figure 1E). As GnT-IVa and GnT-IVb exhibit markedly higher activity toward glycoproteins than free glycans,[18] recognition of substrate proteins by the lectin domain likely contributes to efficient glycosylation of proteins. Furthermore, our previous comprehensive binding analysis revealed that the lectin domain of GnT-IVa preferentially binds to GnT-IV product glycans bearing GlcNAc termini,[17] and GnT-IVa and GnT-IVb tend to be highly active against glycoproteins some of whose glycans have been premodified by GnT-IV.[18] Collectively, these findings imply that recognition of glycoproteins by the lectin domain helps GnT-IVs to efficiently and selectively glycosylate their substrate proteins. Since no reports on the systematic identification of physiological substrate proteins of GnT-IVa or -IVb have been published, exploring GnT-IVa and -IVb substrates *in vivo* could help us understand the details of the mechanism by which GnT-IVa and -IVb select substrates and how their lectin domains are involved in substrate selection.

Although a lectin domain is not common to glycosyltransferases, UDP-GalNAc:polypeptide *N*-acetylgalactosaminyltransferases (GALNTs)[30–32] and protein *O*-linked mannose β1,2-*N*-acetylglucosaminyltransferase 1 (POMGNT1)[33] are other enzymes identified as having a lectin domain to date. In these enzymes, the lectin domain recognizes a product glycan synthesized by the catalytic domain, similar to GnT-IVa and -IVb. The GALNT lectin domain has been proposed to promote efficient and dense glycosylation,[31] while the POMGNT1 lectin domain has been suggested to function by transporting its binding partner enzyme, for example, fukutin, to a specific glycan.[33] Our findings suggest that the GnT-IVa and GnT-IVb lectin domains contribute to raising the efficiency and protein-selectivity of glycosylation. Although the functions of lectin domains could differ among enzymes, their lectin domains commonly recognize the product glycans of catalytic domains. Notably, although Asp and Trp, the two key residues in the glycan binding sites of the GnT-IVa and GnT-IVb lectin domains, are also conserved in GnT-IVc, another critical His residue is not conserved (Figure S11). This suggests that the GnT-IVc lectin domain may bind to different glycan ligands from GnT-IVa and GnT-IVb. As GnT-IVc in chicken and fish was reported to have another type of branching activity toward the α1,6-Man arm,[34] we hypothesize that the lectin domain in the GnT-IV enzyme family might contribute to their different branching activity. Comprehensive glycan binding analysis of GnT-IVa, GnT-IVb, and GnT-IVc lectin domains would reveal how lectin domains in this enzyme family differentially assist glycosylation.

As to the role of GnT-IVa and -IVb *N*-glycans, we found that the structure of a glycan near the glycan recognition site of the lectin domain may regulate catalytic activity toward glycoprotein substrates. Meanwhile, removal of the whole *N*-glycan likely caused partial folding defects (Figure S8). Together with the fact that the *N*-glycosylation site is highly conserved in various species, these findings suggest that the *N*-glycan at this site also plays some roles in forming an active fold of the lectin domain.

Regarding the biological significance of the self-regulation of GnT-IVa and -IVb activity by their own glycans, there are several possibilities. Since GnT-IVa and -IVb activity is negatively regulated, it is possible that the amount of GnT-IVs-produced branching is tightly controlled by this mechanism in cells. Alternatively, this lectin-mediated substrate recognition might prevent aberrant formation of the branching structure in proteins in which it is unwanted. The self-regulatory mechanism might also be related to the precise localization or reaction order of GnT-IVs within the Golgi apparatus. As GnT-IVs are considered to be mainly localized in medial Golgi, its own major *N*-glycan structures are probably Man5 or GlcNAc-terminated glycans, which was confirmed by the glycoproteomic analysis (Figure 3C). Our MD simulation and biochemical

results showed that GnT-IVa and GnT-IVb activity is greater with Man5 glycan than with GlcNAc-terminated complex glycans (Figures 2 and 4). This suggests that GnT-IVs are more active in the cis region of the Golgi than in the medial-trans region, and hence are not equally active throughout the Golgi. This might also be related to the reaction order of glycosyltransferases for *N*-glycan biosynthesis, which is an important factor determining the final structure of *N*-glycans on proteins. In the present study we analyzed the glycan structures of exogenously expressed GnT-IVa and GnT-IVb (Figures 3C and 3D), and it is critically important to determine the *N*-glycan profiles of endogenous GnT-IVa and GnT-IVb in the future.

Another possibility regarding the role of lectin-self ligand interaction is that the lectin domain contributes to forming a homo-dimer by intermolecularly recognizing the glycan ligand. To examine whether GnT-IVa and GnT-IVb form a homo-dimer, we co-expressed myc-tagged and FLAG-tagged enzymes and investigated whether myc-tagged enzyme can be co-precipitated in the anti-FLAG immunoprecipitates. As a result, we found that both GnT-IVa-myc and GnT-IVb-myc can be co-immunoprecipitated with respective FLAG-tagged enzymes (Figure S12), suggesting that GnT-IVa and GnT-IVb form a homo-dimer (or oligomer) in cells. However, prediction of a dimer structure by AlphaFold Multimer suggested that a glycan in a monomer seems to be far from the ligand binding site in the lectin domain of the other monomer (Figure S7). This further supports the idea that the lectin domain interacts with the self ligand intramolecularly but not intermolecularly.

In conclusion, we unveiled that GnT-IVs have unique substrate recognition and self-regulatory mechanisms involving their intramolecular lectin domains, which helps explain protein-selective glycosylation by this enzyme. We recently reported that a non-catalytic domain (N domain) in the luminal region of GnT-V, which forms another branch of *N*-glycan, also plays a critical role in recognizing glycoprotein substrates.[22] Although a GnT-V mutant lacking its N domain also showed the dramatically reduced activity only toward glycoproteins but not toward free glycans, the GnT-V N domain is not a lectin domain and regulates GnT-V activity in a different mode from the GnT-IVs lectin domains. Thus, non-catalytic domains for some glycosyltransferases may commonly have an important role in the selection of glycoprotein substrates. Another important issue is how the lectin domains in GnT-IVa and -IVb coordinate with the catalytic domain during the glycosylation reaction. To clarify this issue, we are now trying to solve the crystal structure that includes both catalytic and lectin domains. We hope that elucidating the whole picture of the regulatory mechanism of GnT-IVs in cells will lead to an understanding of the complex mechanisms by which glycosyltransferases regulate the biosynthesis of *N*-glycans in cells.

Limitations of the study

There are several limitations in this study. First, although we discovered that activity of GnT-IVa and GnT-IVb is regulated by their own glycans, the biological significance of this self-regulation mechanism remains to be clarified. Second, as GnT-IVa and GnT-IVb have multiple *N*-glycosylation sites, the reduction in the activity of glycan-remodeled enzymes toward glycoprotein substrates in Figure 4 might not be solely explained by the role of the specific *N*-glycan in the lectin domain. Third, we tested 4 glycoproteins with multiple *N*-glycans as model substrates and obtained the results which suggested that the lectin domain is indispensable for the activity toward glycoproteins. However, it is unclear whether the importance of the lectin domain can be generally applied to any kind of glycoprotein substrate. It is also unclear how only GnT-IVa D445A mutant among the lectin-dead mutants showed reduced activity toward free glycan substrates.[17] Fourth, our glycoproteomic analysis determined the glycan structures of exogenously expressed GnT-IVa and GnT-IVb, but the glycan structures of endogenous GnT-IVa and GnT-IVb remain unclear due to the low expression levels of the endogenous enzymes.

RESOURCE AVAILABILITY

Lead contact

Further information and requests for resources and reagents should be directed to and will be fulfilled by the lead contact, Y.K. (kizuka.yasuhiko.k8@f.gifu-u.ac.jp).

Material availability

Reagents generated in this study are available from the lead contact with a completed Materials Transfer Agreement.

Data and code availability

- This paper analyzes existing, publicly available data which are listed in the key resources table. The structural data used in this study from the Protein DataBank are listed in the key resources table. Glycoproteomic raw data for glycan structure analysis by LC-ESI MS have been deposited in GlycoPOST and are publicly available. Announced ID is listed in the key resources table.
- No original code was reported in this paper.
- Any additional information required to reanalyze the data reported in this paper is available from the lead contact upon request.

ACKNOWLEDGMENTS

We thank Dr. Taroh Kinoshita (Osaka University) for providing HEK293 SLC35A2 KO cells. We also thank Ms. Emiko Mori (Gifu University) for their technical assistance. We thank Edanz (https://jp.edanz.com/ac) for editing a draft of this manuscript.

This work was supported by a FOREST grant (JPMJFR215Zto Y.K.) from Japan Science and Technology Agency (JST), the Core-to-Core Program (JPJSCCA202000007 to YK) and a Grant-in-Aid for Scientific Research (B) [24K02222 to YK] from the Japan Society for the Promotion of Science (JSPS), an AMED-CREST grant (JP23gm1410011 to Y.K.) from Japan Agency for Medical Research and Development (AMED), the Human Glycome Atlas Project

(HGA) from the Ministry of Education, Culture, Sports, Science and Technology (MEXT), and a grant from the Takeda Science Foundation to Y.K. Computational work was supported by National Institutes of Health (P20GM130460) funding to the Glycoscience Center of Research Excellence.

AUTHOR CONTRIBUTIONS

Conceptualization, Supervision, Project Administration and Funding Acquisition: Y.K.;Formal Analysis: S.K.M. and R.J.D; Investigation: N.O., Y.T., and Mi.N.; Visualization: Ma.N.; Writing – Original Draft: N.O. and Y.K.; Writing – Review and Editing: Y.K. and R.J.D.

DECLARATION OF INTERESTS

The authors declare no competing interests.

STAR★METHODS

Detailed methods are provided in the online version of this paper and include the following:

- KEY RESOURCES TABLE
- EXPERIMENTAL MODEL AND STUDY PARTICIPANT DETAILS
  - Microbe strains
  - Cell lines
- METHOD DETAILS
  - Reagents
  - Plasmid construction
  - Cell culture
  - Plasmid transfection
  - Preparation of cellular and secreted proteins
  - Western and lectin blotting, and CBB staining
  - Purification of recombinant proteins
  - GnT-IV activity assay using HPLC
  - Immunofluorescence staining
  - GnT-IV activity assay using UDP-Glo
  - PNGase F treatment of cell lysate
  - LC-MS glycoproteomic analysis
  - Immunoprecipitation
  - Molecular dynamics simulations
  - Structure presentation
  - Multiple sequence alignment of GnT-IV lectin domains
- QUANTIFICATION AND STATISTICAL ANALYSIS

SUPPLEMENTAL INFORMATION

Supplemental information can be found online at https://doi.org/10.1016/j.isci.2024.111066.

Received: May 4, 2024
Revised: August 1, 2024
Accepted: September 25, 2024
Published: September 28, 2024

REFERENCES

1. Varki, A. (2017). Biological roles of glycans. Glycobiology *27*, 3–49. https://doi.org/10.1093/glycob/cww086.
2. Apweiler, R., Hermjakob, H., and Sharon, N. (1999). On the frequency of protein glycosylation, as deduced from analysis of the SWISS-PROT database. Biochim. Biophys. Acta *1473*, 4–8. https://doi.org/10.1016/S0304-4165(99)00165-8.
3. Moremen, K.W., Tiemeyer, M., and Nairn, A.V. (2012). Vertebrate protein glycosylation: diversity, synthesis and function. Nat. Rev. Mol. Cell Biol. *13*, 448–462. https://doi.org/10.1038/NRM3383.
4. Mereiter, S., Balmaña, M., Campos, D., Gomes, J., and Reis, C.A. (2019). Glycosylation in the Era of Cancer-Targeted Therapy: Where Are We Heading? Cancer Cell *36*, 6–16. https://doi.org/10.1016/J.CCELL.2019.06.006.
5. Ohtsubo, K., Takamatsu, S., Minowa, M.T., Yoshida, A., Takeuchi, M., and Marth, J.D. (2005). Dietary and genetic control of glucose transporter 2 glycosylation promotes insulin secretion in suppressing diabetes. Cell *123*, 1307–1321. https://doi.org/10.1016/J.CELL.2005.09.041.
6. Kizuka, Y., Kitazume, S., Fujinawa, R., Saito, T., Iwata, N., Saido, T.C., Nakano, M., Yamaguchi, Y., Hashimoto, Y., Staufenbiel, M., et al. (2015). An aberrant sugar modification of BACE1 blocks its lysosomal targeting in Alzheimer's disease. EMBO Mol. Med. *7*, 175–189. https://doi.org/10.15252/EMMM.201404438.
7. Stanley, P., Moremen, K.W., Lewis, N.E., Taniguchi, N., and Aebi, M. (2022). N-glycans. In Essentials of Glycobiology [Internet], 4th ed.
8. Aebi, M. (2013). N-linked protein glycosylation in the ER. Biochim. Biophys. Acta *1833*, 2430–2437. https://doi.org/10.1016/J.BBAMCR.2013.04.001.
9. Fisher, P., Thomas-Oates, J., Wood, A.J., and Ungar, D. (2019). The *N*-Glycosylation Processing Potential of the Mammalian Golgi Apparatus. Front. Cell Dev. Biol. *7*, 157. https://doi.org/10.3389/FCELL.2019.00157.
10. Brockhausen, I., Narasimhan, S., and Schachter, H. (1988). The biosynthesis of highly branched N-glycans: studies on the sequential pathway and functional role of N-acetylglucosaminyltransferases I, II, III, IV, V and VI. Biochimie *70*, 1521–1533. https://doi.org/10.1016/0300-9084(88)90289-1.
11. Taniguchi, N., and Kizuka, Y. (2015). Glycans and cancer: role of N-glycans in cancer biomarker, progression and metastasis, and therapeutics. Adv. Cancer Res. *126*, 11–51. https://doi.org/10.1016/BS.ACR.2014.11.001.
12. Minowa, M.T., Oguri, S., Yoshida, A., Hara, T., Iwamatsu, A., Ikenaga, H., and Takeuchi, M. (1998). cDNA cloning and expression of bovine UDP-N-acetylglucosamine: alpha1, 3-D-mannoside beta1,4-N-acetylglucosaminyltransferase IV. J. Biol. Chem. *273*, 11556–11562. https://doi.org/10.1074/JBC.273.19.11556.
13. Sakamoto, Y., Taguchi, T., Honke, K., Korekane, H., Watanabe, H., Tano, Y., Dohmae, N., Takio, K., Horii, A., and

Taniguchi, N. (2000). Molecular cloning and expression of cDNA encoding chicken UDP-N-acetyl-D-glucosamine (GlcNAc): GlcNAcbeta 1-6(GlcNAcbeta 1-2)- manalpha 1-R[GlcNAc to man]beta 1,4N-acetylglucosaminyltransferase VI. J. Biol. Chem. *275*, 36029–36034. https://doi.org/10.1074/JBC.M005860200.

14. Huang, H.H., Hassinen, A., Sundaram, S., Spiess, A.N., Kellokumpu, S., and Stanley, P. (2015). GnT1IP-L specifically inhibits MGAT1 in the Golgi via its luminal domain. Elife *4*, e08916. https://doi.org/10.7554/ELIFE.08916.
15. Ohtsubo, K., Chen, M.Z., Olefsky, J.M., and Marth, J.D. (2011). Pathway to diabetes through attenuation of pancreatic beta cell glycosylation and glucose transport. Nat. Med. *17*, 1067–1075. https://doi.org/10.1038/NM.2414.
16. Yoshida, A., Minowa, M.T., Takamatsu, S., Hara, T., Ikenaga, H., and Takeuchi, M. (1998). A novel second isoenzyme of the human UDP-N-acetylglucosamine:alpha1,3-D-mannoside beta1,4-N-acetylglucosaminyltransferase family: cDNA cloning, expression, and chromosomal assignment. Glycoconj. J. *15*, 1115–1123. https://doi.org/10.1023/A:1006951519522.
17. Nagae, M., Hirata, T., Tateno, H., Mishra, S.K., Manabe, N., Osada, N., Tokoro, Y., Yamaguchi, Y., Doerksen, R.J., Shimizu, T., and Kizuka, Y. (2022). Discovery of a lectin domain that regulates enzyme activity in mouse N-acetylglucosaminyltransferase-IVa (MGAT4A). Commun. Biol. *5*, 695. https://doi.org/10.1038/S42003-022-03661-W.
18. Osada, N., Nagae, M., Nakano, M., Hirata, T., and Kizuka, Y. (2022). Examination of differential glycoprotein preferences of N-acetylglucosaminyltransferase-IV isozymes a and b. J. Biol. Chem. *298*, 102400. https://doi.org/10.1016/J.JBC.2022.102400.
19. Oka, N., Mori, S., Ikegaya, M., Park, E.Y., and Miyazaki, T. (2022). Crystal structure and sugar-binding ability of the C-terminal domain of N-acetylglucosaminyltransferase IV establish a new carbohydrate-binding module family. Glycobiology *32*, 1153–1163. https://doi.org/10.1093/GLYCOB/CWAC058.
20. Takamatsu, S., Korekane, H., Ohtsubo, K., Oguri, S., Park, J.Y., Matsumoto, A., and Taniguchi, N. (2013). N-acetylglucosaminyltransferase (GnT) assays using fluorescent oligosaccharide acceptor substrates: GnT-III, IV, V, and IX (GnT-Vb). Methods Mol. Biol. *1022*, 283–298. https://doi.org/10.1007/978-1-62703-465-4_21.
21. Hirata, T., Nagae, M., Osuka, R.F., Mishra, S.K., Yamada, M., and Kizuka, Y. (2020). Recognition of glycan and protein substrates by N-acetylglucosaminyltransferase-V. Biochim. Biophys. Acta Gen. Subj. *1864*, 129726. https://doi.org/10.1016/J.BBAGEN.2020.129726.
22. Osuka, R.F., Hirata, T., Nagae, M., Nakano, M., Shibata, H., Okamoto, R., and Kizuka, Y. (2022). N-acetylglucosaminyltransferase-V requires a specific noncatalytic luminal domain for its activity toward glycoprotein substrates. J. Biol. Chem. *298*, 101666. https://doi.org/10.1016/J.JBC.2022.101666.
23. Dela Cruz, C.S., Lee, Y., Viswanathan, S.R., El-Guindy, A.S., Gerlach, J., Nikiforow, S., Shedd, D., Gradoville, L., and Miller, G. (2004). N-linked Glycosylation Is Required for Optimal Function of Kaposi's Sarcoma Herpesvirus–encoded, but Not Cellular, Interleukin 6. J. Exp. Med. *199*, 503–514. https://doi.org/10.1084/JEM.20031205.
24. Ioffe, E., and Stanley, P. (1994). Mice lacking N-acetylglucosaminyltransferase I activity die at mid-gestation, revealing an essential role for complex or hybrid N-linked carbohydrates. Proc. Natl. Acad. Sci. USA *91*, 728–732. https://doi.org/10.1073/PNAS.91.2.728.
25. Goldstein, I.J., Reichert, C.M., and Misaki, A. (1974). Interaction of concanavalin A with model substrates. Ann. N. Y. Acad. Sci. *234*, 283–296. https://doi.org/10.1111/J.1749-6632.1974.TB53040.X.
26. Crowley, J.F., Goldstein, I.J., Arnarp, J., and Lönngren, J. (1984). Carbohydrate binding studies on the lectin from Datura stramonium seeds. Arch. Biochem. Biophys. *231*, 524–533. https://doi.org/10.1016/0003-9861(84)90417-X.
27. Bhattacharyya, L., Haraldsson, M., and Brewer, C.F. (1988). Precipitation of galactose-specific lectins by complex-type oligosaccharides and glycopeptides: studies with lectins from Ricinus communis (agglutinin I), Erythrina indica, Erythrina arborescens, Abrus precatorius (agglutinin), and Glycine max (soybean). Biochemistry *27*, 1034–1041. https://doi.org/10.1021/BI00403A028.
28. Hirata, T., Takata, M., Tokoro, Y., Nakano, M., and Kizuka, Y. (2022). Shedding of N-acetylglucosaminyltransferase-V is regulated by maturity of cellular N-glycan. Commun. Biol. *5*, 743. https://doi.org/10.1038/s42003-022-03697-y.
29. Zhu, K., Bressan, R.A., Hasegawa, P.M., and Murdock, L.L. (1996). Identification of N-acetylglucosamine binding residues in Griffonia simplicifolia lectin II. FEBS Lett. *390*, 271–274. https://doi.org/10.1016/0014-5793(96)00671-0.
30. Fritz, T.A., Hurley, J.H., Trinh, L.B., Shiloach, J., and Tabak, L.A. (2004). The beginnings of mucin biosynthesis: the crystal structure of UDP-GalNAc:polypeptide alpha-N-acetylgalactosaminyltransferase-T1. Proc. Natl. Acad. Sci. USA *101*, 15307–15312. https://doi.org/10.1073/PNAS.0405657101.
31. Kubota, T., Shiba, T., Sugioka, S., Furukawa, S., Sawaki, H., Kato, R., Wakatsuki, S., and Narimatsu, H. (2006). Structural basis of carbohydrate transfer activity by human UDP-GalNAc: polypeptide alpha-N-acetylgalactosaminyltransferase (pp-GalNAc-T10). J. Mol. Biol. *359*, 708–727. https://doi.org/10.1016/J.JMB.2006.03.061.
32. Kong, Y., Joshi, H.J., Schjoldager, K.T.B.G., Madsen, T.D., Gerken, T.A., Vester-Christensen, M.B., Wandall, H.H., Bennett, E.P., Levery, S.B., Vakhrushev, S.Y., and Clausen, H. (2015). Probing polypeptide GalNAc-transferase isoform substrate specificities by in vitro analysis. Glycobiology *25*, 55–65. https://doi.org/10.1093/GLYCOB/CWU089.
33. Kuwabara, N., Manya, H., Yamada, T., Tateno, H., Kanagawa, M., Kobayashi, K., Akasaka-Manya, K., Hirose, Y., Mizuno, M., Ikeguchi, M., et al. (2016). Carbohydrate-binding domain of the POMGnT1 stem region modulates O-mannosylation sites of α-dystroglycan. Proc. Natl. Acad. Sci. USA *113*, 9280–9285. https://doi.org/10.1073/PNAS.1525545113.
34. Taguchi, T., Ogawa, T., Inoue, S., Inoue, Y., Sakamoto, Y., Korekane, H., and Taniguchi, N. (2000). Purification and characterization of UDP-GlcNAc: GlcNAcbeta 1-6(GlcNAcbeta 1-2)Manalpha 1-R [GlcNAc to Man]-beta 1, 4-N-acetylglucosaminyltransferase VI from hen oviduct. J. Biol. Chem. *275*, 32598–32602. https://doi.org/10.1074/JBC.M004673200.
35. Case, D.A., Aktulga, H.M., Belfon, K., Cerutti, D.S., Cisneros, G.A., Cruzeiro, V.W.D., Forouzesh, N., Giese, T.J., Götz, A.W., Gohlke, H., et al. (2023). AmberTools. J. Chem. Inf. Model. *63*, 6183–6191. https://doi.org/10.1021/ACS.JCIM.3C01153.
36. Woods, R.J. coworkers GLYCAM Web. http://glycam.org/. Accessed 01-08-2014.
37. Maier, J.A., Martinez, C., Kasavajhala, K., Wickstrom, L., Hauser, K.E., and Simmerling, C. (2015). ff1$_4$SB: Improving the accuracy of protein side chain and backbone parameters from ff$_{99}$SB TOC figure HHS Public Access. J. Chem. Theor. Comput. *11*, 3696–3713. https://doi.org/10.1021/acs.jctc.5b00255.
38. Kirschner, K.N., Yongye, A.B., Tschampel, S.M., González-Outeiriño, J., Daniels, C.R., Foley, B.L., and Woods, R.J. (2008). GLYCAM06: a generalizable biomolecular force field. J. Comput. Chem. *29*, 622–655. https://doi.org/10.1002/JCC.20820.
39. Roe, D.R., and Cheatham, T.E. (2013). PTRAJ and CPPTRAJ: Software for Processing and Analysis of Molecular Dynamics Trajectory Data. J. Chem. Theor. Comput. *9*, 3084–3095. https://doi.org/10.1021/CT400341P.
40. Humphrey, W., Dalke, A., and Schulten, K. (1996). VMD: Visual molecular dynamics. J. Mol. Graph. *14*, 33–38. https://doi.org/10.1016/0263-7855(96)00018-5.
41. Schrödinger, L., and DeLano, W. (2022). PyMOL. http://www.pymol.org/pymol.
42. Jumper, J., Evans, R., Pritzel, A., Green, T., Figurnov, M., Ronneberger, O., Tunyasuvunakool, K., Bates, R., Žídek, A., Potapenko, A., et al. (2021). Highly accurate protein structure prediction with AlphaFold. Nature *596*, 583–589. https://doi.org/10.1038/S41586-021-03819-2.
43. Krissinel, E., and Henrick, K. (2004). Secondary-structure matching (SSM), a new tool for fast protein structure alignment in three dimensions. Acta Crystallogr. D Biol. Crystallogr. *60*, 2256–2268. https://doi.org/10.1107/S0907444904026460.
44. Wang, Y., Hirata, T., Maeda, Y., Murakami, Y., Fujita, M., and Kinoshita, T. (2019). Free, unlinked glycosylphosphatidylinositols on mammalian cell surfaces revisited. J. Biol. Chem. *294*, 5038–5049. https://doi.org/10.1074/JBC.RA119.007472.
45. Takahashi, S., Sugiyama, T., Shimomura, M., Kamada, Y., Fujita, K., Nonomura, N., Miyoshi, E., and Nakano, M. (2016). Site-specific and linkage analyses of fucosylated N-glycans on haptoglobin in sera of patients with various types of cancer: possible implication for the differential diagnosis of cancer. Glycoconj. J. *33*, 471–482. https://doi.org/10.1007/S10719-016-9653-7.
46. Nagae, M., Mishra, S.K., Hanashima, S., Tateno, H., and Yamaguchi, Y. (2017). Distinct roles for each N-glycan branch interacting with mannose-binding type Jacalin-related lectins Orysata and Calsepa. Glycobiology

27, 1120–1133. https://doi.org/10.1093/GLYCOB/CWX081.

47. Loncharich, R.J., Brooks, B.R., and Pastor, R.W. (1992). Langevin dynamics of peptides: the frictional dependence of isomerization rates of N-acetylalanyl-N′-methylamide. Biopolymers *32*, 523–535. https://doi.org/10.1002/BIP.360320508.

48. Henrich, S., Cameron, A., Bourenkov, G.P., Kiefersauer, R., Huber, R., Lindberg, I., Bode, W., and Than, M.E. (2003). The crystal structure of the proprotein processing proteinase furin explains its stringent specificity. Nat. Struct. Biol. *10*, 520–526. https://doi.org/10.1038/NSB941.

49. Thompson, J.D., Higgins, D.G., and Gibson, T.J. (1994). CLUSTAL W: improving the sensitivity of progressive multiple sequence alignment through sequence weighting, position-specific gap penalties and weight matrix choice. Nucleic Acids Res. *22*, 4673–4680. https://doi.org/10.1093/NAR/22.22.4673.

STAR★METHODS

KEY RESOURCES TABLE

REAGENT or RESOURCE	SOURCE	IDENTIFIER
Antibodies and lectins		
Mouse anti-myc (4A6)	Millipore	Cat#05-724; RRID: AB_309938
Rabbit anti-FLAG	Cell Signaling	Cat#14793; RRID: AB_2572291
Rabbit anti-GnT-IVa	Proteintech	Cat#25109-1-AP; RRID: AB_2879901
Rabbit anti-GnT-IVb	Novus Biologicals	Cat#NBP3-05020; RRID: AB_3533192
Mouse anti-GAPDH (6C5)	Millipore	Cat#MAB374; RRID: AB_2107445
Rabbit anti-Haptoglobin	Abcam	Cat#Ab256454; RRID: AB_2892593
Rabbit anti-Golgin-97 (D8P2K)	Cell Signaling	Cat#13192S; RRID: AB_2798144
HRP-*anti*-mouse IgG	GE Healthcare	Cat#NA931A; RRID: AB_772210
HRP-*anti*-rabbit IgG	GE Healthcare	Cat#NA934V; RRID: AB_772206
Alexa 546-*anti*-rabbit IgG	Invitrogen	Cat#A10040; RRID: AB_2534016
Alexa 488-*anti*-mouse IgG	Invitrogen	Cat#A21202; RRID: AB_141607
DSA	J-Chemical	Cat#J105
Biotinylated RCA	Vector Laboratories	Cat#B-1085
Biotinylated GSLII	Vector Laboratories	Cat#B-1215
Biotinylated ConA	J-Chemical	Cat#J203
Bacterial and virus strains		
XL-10 Gold Ultracompetent cells	Agilent Technologies	Cat#200315
DH5-alpha competent cells	TAKARA	Cat#9057
Chemicals, peptides, and recombinant proteins		
PNGase F	New England Biolabs	Cat#P0704L
Neuraminidase	Nacalai Tesque	Cat#24229-74
Beta1-4 galactosidase S	New England Biolabs	Cat#0745L
Protease inhibitor cocktail set V (EDTA-free)	Fujifilm	Cat#168-26033
Lipofectamine 3000	ThermoFisher Scientific	Cat#L3000
Polyethylenimine (PEI) MAX	Polysciences	Cat#24765
ExpiFectamine 293	ThermoFisher Scientific	Cat#A14524
NEBuilder HiFi DNA Assembly Master Mix	New England Biolabs	Cat#E2621
GnGnbi-PA	Takamatsu et al.[20]	N/A
GelCode Blue Safe Protein Stain	ThermoFisher Scientific	Cat#24594
Dynabeads Protein G	Invitrogen	Cat#DB10004
Anti-DYKDDDDK tag antibody magnetic beads	Fujifilm	Cat#017-25151
Streptavidin FG beads	Tamagawa	Cat#TAS8848N1170
Human α1AGP	Sigma	Cat#G9885
Human haptoglobin	Sigma	Cat#H3536
Human α1-antitrypsin	Sigma	Cat#A9024
Human interleukin-6	Abcam	Cat#ab259381
Ultra Pure UDP-GlcNAc (for UDP-Glo assay)	Promega	Cat#V7072
Critical commercial assays		
Peroxidase Labeling Kit-NH2	Dojindo	LK11
QuikChange Lightning Site-Directed Mutagenesis kit	Agilent Technologies	Cat#210518-5

(*Continued on next page*)

Continued

REAGENT or RESOURCE	SOURCE	IDENTIFIER
Pierce BCA Protein Assay Kit	ThermoFisher Scientific	Cat#23227
VECTASTAIN ABC Standard Kit	Vector Laboratories	PK-4000
UDP-Glo Glycosyltransferase Assay Kit	Promega	Cat#V6962
Deposited data		
LC-MS glycoproteomic data	https://glycopost.glycosmos.org/	GPST000385
Structure of mouse GnT-IVa lectin domain	Protein DataBank	PDB ID: 7VMT
Structure of mouse furin	Protein DataBank	PDB ID: 1P8J
Structure of B.mori GnT-IV lectin domain	Protein DataBank	PDB ID: 7XTN
Experimental models: Cell lines		
COS7	RIKEN Cell bank	RCB0539
HEK293	ATCC	CRL-1573
HEK293-GnT-IVa/GnT-IVb-DKO	Nagae et al.[17]	N/A
HEK293-SLC35A2-KO	Hirata et al.[28]	N/A
Expi293F	ThermoFisher Scientific	Cat#A14527
Expi293-GnT-I-KO	ThermoFisher Scientific	Cat#A39240
Oligonucleotides		
Primers for constructing the plasmids, see Table S4	This study	N/A
Recombinant DNA		
pcDNA6 myc-His A/mouse GnT-IVa	Nagae et al.[17]	N/A
pcDNA6 myc-His A/mouse GnT-IVb	Osada et al.[18]	N/A
pcDNA-IH/mouse GnT-IVa	Nagae et al.[17]	N/A
pcDNA-IH/mouse GnT-IVa D445A	Nagae et al.[17]	N/A
pcDNA-IH/mouse GnT-IVb	Osada et al.[18]	N/A
pcDNA6 myc-His A/mouse GnT-IVa N79A	This study	N/A
pcDNA6 myc-His A/mouse GnT-IVa N449S	This study	N/A
pcDNA6 myc-His A/mouse GnT-IVa W513A	This study	N/A
pcDNA-IH/mouse GnT-IVa W513A	This study	N/A
pcDNA6 myc-His A/mouse GnT-IVb N87S	This study	N/A
pcDNA6 myc-His A/mouse GnT-IVb N103S	This study	N/A
pcDNA6 myc-His A/mouse GnT-IVb N465S	This study	N/A
pcDNA-IH/mouse GnT-IVb D461A	This study	N/A
pcDNA-IH/mouse GnT-IVb W536A	This study	N/A
pME-3xFLAG/mouse GnT-IVa	This study	N/A
pME-3xFLAG/mouse GnT-IVb	This study	N/A
Software and algorithms		
GlycoMod	SIB Swiss Institute of Bioinformatics	https://web.expasy.org/glycomod
Xcalibur	ThermoFisher Scientific	N/A
LCSolution	Shimadzu	N/A
BZ-X800 analyzer	Keyence	N/A
ClustalW	Kyoto University Bioinformatics Center	https://www.genome.jp/tools-bin/clustalw
ImageJ Fiji	GitHub	https://Fiji.sc
AmberTools20	Case et al.[35]	https://ambermd.org
AmberTools22	Case et al.[35]	https://ambermd.org
Glycam-web	Woods et al.[36]	http://glycam.org/

(*Continued on next page*)

Continued

REAGENT or RESOURCE	SOURCE	IDENTIFIER
ff14SB	Maier et al.[37]	N/A
Glycam06 (version J1)	Kirschner et al.[38]	N/A
cpptraj	Roe et al.[39]	N/A
VMD	Humphrey et al.[40]	N/A
PyMOL	Schrodinger et al.[41]	https://www.pymol.org
AlphaFold2	Jumper et al.[42]	https://alphafold.ebi.ac.uk
GraphPad Prism 8 software	GraphPad Software, Inc.	https://www.graphpad.com
SUPERPOSE	Krissinel et al.[43]	N/A

EXPERIMENTAL MODEL AND STUDY PARTICIPANT DETAILS

Microbe strains

We used XL-10 Gold Ultracompetent cells (Agilent Technologies) and DH5-alpha competent cells (TAKARA) for plasmid construction.

Cell lines

All cell lines used in this study for cellular assays are listed in the key resources table. COS7 cells were obtained from RIKEN Cell bank, and HEK293 cells were obtained from the American Type Culture Collection. Expi293F and Expi293-GnT-I-KO cells were obtained from ThermoFisher Scientific. All cell lines were verified to be free of mycoplasma contamination.

METHOD DETAILS

Reagents

The following antibodies and lectins were used: anti-myc (mouse, clone 4A6; Millipore; catalog no.: 05–724), anti-FLAG (rabbit; Cell Signaling; catalog no.: 14793), anti-GnT-IVa (rabbit; Proteintech; catalog no.: 25109-1-AP), anti-GnT-IVb (rabbit; Novus Biologicals; catalog no.: NBP3-05020), anti-GAPDH (mouse, clone 6C5; Merck Millipore; catalog no.: MAB374), anti-Haptoglobin (rabbit, Abcam; catalog no.: ab256454), anti-Golgin-97 (rabbit, clone D8P2K, Cell Signaling Technology; catalog no.: 13192S), horseradish peroxidase (HRP)-conjugated anti-mouse IgG (GE Healthcare; catalog no.: NA931V), HRP-conjugated anti-rabbit IgG (GE Healthcare; catalog no.: NA934V), DSA (J-Chemical; catalog no.: J105), biotinylated RCA (Vector Laboratories; catalog no.: B-1085), biotinylated GSLII (Vector Laboratories; catalog no.: B-1215), biotinylated ConA (J-Chemical; catalog no.: J203), Alexa 546-conjugated anti-rabbit IgG (Invitrogen; catalog no.: A10040), and Alexa 488-conjugated anti-mouse IgG (Invitrogen; catalog no.: A21202). DSA was conjugated to HRP using a Peroxidase Labeling Kit-NH_2 (Dojindo), in accordance with the manufacturer's protocol. Recombinant human IL-6 was purchased from Abcam (catalog no.: ab259381).

Plasmid construction

Primers used in this study are listed in Table S4 pcDNA6 myc-His A/mouse GnT-IVa (UniProt ID: Q812G0-2), pcDNA6 myc-His A/mouse GnT-IVb (UniProt ID: Q812G0-2), the plasmids for 6×His-tagged soluble mouse GnT-IVa (pcDNA-IH/GnT-IVa) and its mutant (pcDNA-IH/GnT-IVa D445A), and mouse GnT-IVb (pcDNA-IH/GnT-IVb) were constructed as described previously.[17,18] The plasmids for the point mutants of GnT-IVa (N79A, D445A, N449S, W513A) or GnT-IVb (N87S, N103S, D461A, N465S, W536A) were constructed using pcDNA6 myc-His A/mouse GnT-IVa, pcDNA6 myc-His A/mouse GnT-IVb, pcDNA-IH/GnT-IVa, and pcDNA-IH/GnT-IVb as a template and the QuikChange Lightning Site-Directed Mutagenesis Kit (Agilent Technologies), in accordance with the manufacturer's protocol. The reason for choosing Ala instead of Ser at N79 in GnT-IVa was to avoid generation of an additional artificial *N*-glycosylation site at N77. For construction of pME-3×FLAG/mGnT-IVa and pME-3×FLAG/mGnT-IVb, cDNA encoding mouse GnT-IVa or GnT-IVb was amplified by PCR using the pcDNA6 myc-His A/mouse GnT-IVa or GnT-IVb as a template. The PCR products were digested with XhoI-MluI (GnT-IVa) or EcoRI-MluI (GnT-IVb) and then inserted to the XhoI-MluI or EcoRI-MluI sites of pME-3×FLAG.

Cell culture

COS7, HEK293, HEK293 GnT-IVa, GnT-IVb DKO, and HEK293 SLC35A2 KO cells were cultured in Dulbecco's modified Eagle's medium containing 10% fetal bovine serum and 50 μg/mL kanamycin under 5% CO_2 conditions at 37°C HEK293 GnT-IVa, GnT-IVb DKO, and HEK293 SLC35A2 KO cell clones were established using the CRISPR/Cas9 system, as described previously.[17,28,44] Expi 293F (Thermo Fisher Scientific) and Expi 293 GnT-I KO (Thermo Fisher Scientific) cells were cultured in Expi293 Expression Medium under 8% CO_2 conditions at 37°C in a shaking incubator at 120 rpm.

Plasmid transfection

In accordance with the manufacturer's protocol, cells at 70%–80% confluence on a 6-cm dish were transfected with 2 μg of plasmids using Lipofectamine 3000 reagent (Thermo Fisher Scientific). Cells were collected 48 h after transfection and used for subsequent experiments. For the expression of recombinant soluble GnT-IVs, polyethyleneimine MAX (Polysciences) was used, as described below (see "purification of recombinant proteins" section).

Preparation of cellular and secreted proteins

Cells were washed with PBS and collected by centrifugation at 410*g* for 5 min. The cells were washed again with PBS and centrifuged at 13,800 g for 1 min. The cells were lysed with lysis buffer [50 mM Tris–HCl (pH 7.4), 150 mM NaCl, 1% Nonidet P-40, Protease Inhibitor Cocktail Set V (EDTA-free) (Fujifilm)] and sonicated. The protein concentrations of the cell lysates were measured using the Pierce BCA Protein Assay Kit (Thermo Fisher Scientific), in accordance with the manufacturer's protocol. Lysates or protein solution samples for SDS-PAGE analysis were prepared by mixing these samples with Laemmli 5× SDS sample buffer and boiling the samples at 95°C for 5 min.

To analyze secreted proteins, the media were collected and concentrated by 8-fold using Amicon Ultra-4 Centrifugal Filter Devices (Millipore). The samples of concentrated media for SDS-PAGE analysis were prepared by mixing these samples with Laemmli 5× SDS sample buffer and boiling the samples at 95°C for 5 min.

Western and lectin blotting, and CBB staining

The same amount of protein was loaded into each lane of the SDS-PAGE gel, and the proteins were separated by 5%–20% SDS-PAGE. For CBB staining of the gel, the proteins were stained with GelCode Blue Safe Protein Stain (Thermo Fisher Scientific) and visualized using FUSION-SOLO 7s EDGE (Vilber–Lourmat). For western blotting, the proteins separated in the gel were transferred to nitrocellulose membranes using a semi-dry blotter. The membranes were blocked with 5% skim milk in Tris-buffered saline (TBS) containing 0.1% Tween 20 (TBS-T) and incubated with primary antibodies diluted with 5% skim milk in TBS-T overnight at 4°C. After washing with TBS-T for 5 min three times, the membranes were incubated with HRP-conjugated secondary antibodies at room temperature for 1 h. For blotting with HRP lectins, membranes were blocked with 1% BSA in TBS-T overnight at 4°C, followed by incubation at room temperature for 1 h with HRP-conjugated lectins that were diluted with 1% BSA in TBS-T. For blotting with biotinylated lectins, membranes were blocked with TBS-T overnight at 4°C, followed by incubation at room temperature for 30 min with biotinylated lectins diluted with TBS-T. After washing with TBS, the membranes were incubated with the VECTASTAIN ABC Standard kit (Vector Laboratories) (1:400 dilution in TBS-T) at room temperature for 30 min. Signals were detected with the Western Lightning Plus-ECL (PerkinElmer) using FUSION-SOLO 7s EDGE.

Purification of recombinant proteins

COS7 cells were cultured on 15-cm dishes to obtain soluble His-tagged GnT-IVa and GnT-IVb and their lectin domain point mutants. Cells were transfected with the plasmids using poly-ethyleneimine MAX (Polyscience) when confluence reached 70%–80%. After 4–6 h, the medium was replaced with Opti-MEM I, followed by further incubation for 72 h. Soluble His-tagged GnT-IVs were purified from the medium using a Ni^{2+} column. After washing the column with 10 mM phosphate buffer (pH 7.4) containing 20 mM imidazole and 0.5 M NaCl, the recombinant proteins were eluted with 10 mM phosphate buffer (pH 7.4) containing 0.5 M imidazole and 0.5 M NaCl (elution buffer), followed by desalting using a NAP-5 gel filtration column (GE Healthcare). The eluates were used directly as the enzyme sources.

For the expression of proteins in Expi293F and Expi293 GnT-I KO cells, cells were seeded at a density of 3×10^6 viable cells/mL and transfected with 15 μg of plasmids using ExpiFectamine 293 Reagent (Thermo Fisher Scientific). After 18–22 h of transfection, ExpiFectamine 293 Transfection Enhancer 1 and ExpiFectamine 293 Transfection Enhancer 2 were added, in accordance with the manufacturer's protocol. The culture supernatants were collected 5 days after transfection, centrifuged at 410 g for 5 min, and dialyzed overnight against PBS. The dialyzed media were centrifuged at 720 g for 10 min, and the supernatant was filtrated with 0.45 μm PVDF filter. Soluble His-tagged GnT-IV was purified from the media using a Ni^{2+} column as described above.

GnT-IV activity assay using HPLC

GnT-IV activity toward an oligosaccharide substrate was measured using HPLC, as described previously,[20] with slight modifications. In brief, the fluorescence-labeled oligosaccharide GnGnbi-PA (pyridylamine) was used as the substrate, and cell lysates or purified soluble His-tagged GnT-IVs were used as the enzyme source. The enzyme source was incubated at 37°C in 10 μL of reaction buffer, which contained 10 μM GnGnbi-PA, 20 mM UDP-GlcNAc, 25 mM MES (pH 7.7), 0.5% (v/v) Triton X-100, 5 mg/mL BSA, and 7.5 mM $MnCl_2$. The GnT-IV reaction was stopped by boiling at 95°C for 5 min, and 40 μL of water was added to the mixture. After centrifugation at 16,000 g for 5 min, the supernatant was analyzed by reversed-phase HPLC equipped with an ODS column (Inertsil ODS-3, GL Sciences, 4.6 × 250 mm). HPLC analysis was conducted in the isocratic mode with buffers A [20 mM ammonium acetate buffer (pH 4.0)] and B (1% 1-butanol in buffer A) mixed at a ratio of 4:1.

Immunofluorescence staining

Cells seeded on an eight-well glass chamber slide were transfected with 0.1 μg of plasmid using Lipofectamine 3000 transfection reagent. After 48 h, the cells were washed with PBS and fixed with 4% paraformaldehyde/PBS for 15 min at room temperature. The cells were washed

with PBS and then permeabilized by incubating with PBS containing 0.1% Nonidet P-40 and 3% BSA for 30 min. After washing with PBS, the cells were incubated with primary antibodies for 1 h at room temperature, followed by incubation with Alexa 488-or Alexa 546-conjugated secondary antibodies and 4′,6- diamidino-2-phenylindole (DAPI). Fluorescence signals were visualized using a BZX-800 all-in-one fluorescence microscope (KEYENCE). The intensity was quantified using ImageJ Fiji software (https://Fiji.sc): the acquired images were converted to 8 bit and the outlines of the Golgin-97 signals within them were determined, after which the R values as Pearson's correlation coefficients between the Golgin-97 and Myc signals in the enclosed parts were calculated by Coloc 2.

GnT-IV activity assay using UDP-Glo

To prepare asialoagalacto acceptor substrates, human α1AGP (Sigma; catalog no.: G9885), human haptoglobin (Sigma; catalog no.: H3536), human α1-antitrypsin (Sigma; catalog no.: A9024), and human IL-6 (Abcam; catalog no.: ab259381) were digested with neuraminidase (Nacalai Tesque) and β-galactosidase (New England Biolabs), as described previously.[18] The UDP-Glo assay was performed using a UDP-Glo Glycosyltransferase Assay kit (Promega), as described previously.[21] Briefly, the GnT-IV reaction was conducted in a 96-well white plate by incubating purified GnT-IVs with acceptor asialoagalacto substrates for 2 h at room temperature (or 37°C for IL-6) in a 10 μL reaction mixture, which contained 10 mM ultrapure UDP-GlcNAc (Promega), an acceptor substrate, 25 mM MES (pH 7.7), 0.5% (v/v) Triton X-100, 5 mg/mL BSA, and 7.5 mM $MnCl_2$. The concentrations of the acceptor substrates were defined so that 100 pmol of *N*-glycans were added per well based on the number of *N*-glycans they have (α1AGP, 5; haptoglobin, 4; α1-antitrypsin, 3; IL-6, 1). After the reaction, 15 μL of the GnT-IV buffer {25 mM MES (pH 7.7), 0.5% [v/v] Triton X-100, 5 mg/mL BSA, and 7.5 mM $MnCl_2$} was added to each well, followed by adding 25 μL of the UDP detection reagent (supplied in the kit). Then, the plate was incubated in the dark for 1 h at room temperature. Chemiluminescence signals were measured using an SYNERGY H1 microplate reader (BioTek). Duplicate measurements were performed for each sample.

For separating glycoforms of GnT-IVa, soluble His-tagged GnT-IVa was first expressed in HEK293 GnT-IVa and GnT-IVb DKO cells and purified from the culture medium using a Ni^{2+}-column as described above (see "purification of recombinant proteins"). Purified GnT-IVa was incubated with biotinylated RCA or GSLII with Streptavidin FG magnetic beads (Tamagawa) at 4°C overnight. The beads were washed twice with 0.1% Nonidet P-40/TBS and then directly used for UDP-Glo assay as an enzyme source.

PNGase F treatment of cell lysate

For PNGase F treatment, the cells were lysed with lysis buffer [50 mM Tris–HCl (pH 7.4), 150 mM NaCl, 1% Nonidet P-40, Protease Inhibitor Cocktail Set V (EDTA free) (Fujifilm)] and sonicated. The cell lysate samples were denatured in the presence of 0.5% SDS at 95°C for 5 min, followed by 5-fold dilution with TBS containing Nonidet P-40 (final concentration of 0.5%). Two microliters of PNGase F (New England Biolabs) or water (negative control) was added, followed by incubation at 37°C for 2 h. The samples were then mixed with Laemmli 5× SDS sample buffer and incubated at 95°C for 5 min for SDS-PAGE.

LC-MS glycoproteomic analysis

HEK293 GnT-IVa and GnT-IVb DKO cells were cultured on 15-cm dishes and transiently transfected with plasmids encoding full-length myc-his-tagged GnT-IVa or GnT-IVb. Cells were washed with PBS and collected by centrifugation at 410*g* for 5 min. The cells were washed again with PBS and centrifuged at 13,800 g for 1 min. The cells were lysed with lysis buffer [50 mM Tris–HCl (pH 7.4), 150 mM NaCl, 1% Nonidet P-40, Protease Inhibitor Cocktail Set V (EDTA-free) (Fujifilm)] and sonicated. The cell lysates were ultracentrifuged at 100,000 g for 15 min. The supernatants were collected and incubated with anti-Myc antibody and Dynabeads Protein G (Thermo Fisher Scientific) at 4°C overnight. The beads were washed three times with 0.1% Nonidet P-40/TBS, and the bound proteins were eluted by Laemmli 1× SDS sample buffer and incubated at 95°C for 5 min. The samples were separated by SDS-PAGE and stained with GelCode Blue Safe Protein Stain. Bands of GnT-IVa or -IVb were cut and destained with 30% acetonitrile containing 5 mM ammonium bicarbonate three times for 5 min each, followed by further destaining with 100% acetonitrile three times for 5 min each. After destaining, the samples were dried in desiccators. Proteins in the gel bands were digested with trypsin after reduction with dithiothreitol and alkylation with iodoacetamide. Tryptic peptides extracted from gel bands with 0.1% TFA in 50% acetonitrile and 0.1% TFA in 10% acetonitrile were dried using SpeedVac for subsequent LC-MS analysis.[45]

The soluble forms of GnT-IVa and -IVb were purified from the culture media of HEK293 GnT-IVa and GnT-IVb DKO cells using Ni^{2+}-Sepharose, as described in the "purification of recombinant proteins" section. After desalting using a NAP-5 gel filtration column, the eluates were evaporated using SpeedVac. The purified proteins were dissolved in a denaturing solution, reduced with dithiothreitol, and then alkylated with iodoacetamide. The proteins were digested with trypsin after desalting using a NAP-5 gel filtration column, in accordance with previously reported procedures.[45] Tryptic peptides were dried using SpeedVac for subsequent LC-MS analysis.[45]

Monoisotopic masses were assigned with possible monosaccharide compositions on peptides using the GlycoMod software tool (mass tolerance for precursor ions of ±0.01 Da; https://web.expasy.org/glycomod/). Xcalibur software, version 2.2 (Thermo Fisher Scientific), was used to show the base peak chromatogram (BPC), extracted ion chromatogram (EIC), and average mass spectrum (Ave. MS) to analyze MS and MS/MS data. The relative abundances (%) of each glycan structure on each peptide were calculated by setting the total peak intensities of all detected glycopeptides on each *N*-glycan binding site in each EIC as 100%.

Immunoprecipitation

Cells were suspended in lysis buffer (50 mM Tris–HCl [pH 7.4], 150 mM NaCl, 1% Nonidet P-40, Protease Inhibitor Cocktail Set V [EDTA free] [Fujifilm]) and lysed with sonication. The cell lysates were ultracentrifuged at 100,000 g for 15 min, and the supernatants were collected. An aliquot of the collected supernatant was used as input for Western blotting and the rest was incubated with Anti-DYKDDDDK tag Antibody magnetic beads (FUJIFILM) at 4°C overnight. The beads were washed three times with 0.1% Nonidet P-40/TBS and then boiled with 2× Laemmli SDS sample buffer at 95°C for 5 min to elute the proteins bound to the beads.

Molecular dynamics simulations

The protein structure was obtained from the Protein DataBank (PDB ID: 7VMT)[17] and prepared using the program *tleap* in AmberTools20.[35] The lectin domain was glycosylated with eight different *N*-glycans consisting of oligomannose (#005), agalactosylated (#103, 105), galactosylated (#307, 313), and sialylated (#503, 504, 506) *N*-glycans reported previously[17] on N449 of mouse GnT-IVa. These *N*-glycans were modeled and attached to N449 using the glycoprotein builder of Glycam-web.[36] The glycoprotein was solvated in an octahedral TIP3P water box extending 12 Å in each direction from the protein. Sodium ions (Na^+) were introduced to neutralize the overall charge of the system. The protein was parameterized using ff14SB,[37] while the glycans were modeled using the Glycam06 (version J1)[38] force field.

Prepared systems were subjected to a previously published multistep equilibration protocol, consisting of minimization, heating to 300 K, and density equilibration.[46] Finally, microsecond-long MD simulations in the NPT ensemble were performed for each system using the cuda version of *pmemd* in Amber20.[35] The simulations used a time step of 2 fs, periodic boundary conditions, and a Langevin thermostat[47] with a collision frequency of 2 ps^{-1} to maintain a temperature of 300 K. Non-bonded interactions were evaluated using a 9 Å cut-off, and coordinates were saved every 100 ps in the trajectory. A 1 μs MD simulation was conducted for each case, except for 005, 103, 105, and 307, for which the MD simulations were extended to 2 μs to ensure that sufficient sampling was achieved.

Further post processing of each MD trajectory to calculate the grid density of the *N*-glycans was carried out using the *cpptraj*[39] module of AmberTools22.[35] All MD frames were aligned to the first MD frame, and the 'grid' command was used to calculate the grid density of the *N*-glycan heavy atoms on a 3D grid with 50 grid bins and 0.5 Å spacing in each dimension. The MD trajectories and densities were visualized using VMD[40] and PyMOL.[41] The free-energy maps of the *N*-glycan conformations were calculated using in-house scripts.

Structure presentation

All structural coordinates were retrieved from the Protein DataBank (PDB). Structural superpositions were performed with the program SUPERPOSE.[43] Putative 3D structures of murine GnT-IVa and GnT-IVb luminal domains were generated with the program AlphaFold2.[42] The 3D structures of complex-type *N*-glycans were extracted from the atomic coordinates of furin (PDB code: 1P8J).[48] The extracted glycan and stem asparagine residues were superimposed onto potential *N*-glycosylation sites of GnT-IVa and GnT-IVb. Structures were visualized using PyMOL v2.0 (The PyMOL Molecular Graphics System, Version 2.0, Schrödinger, LLC).

Multiple sequence alignment of GnT-IV lectin domains

All amino acid sequences of GnT-IVa and GnT-IVb were retrieved from the UniProtKB database. Multiple amino acid sequence alignment was performed with the ClustalW server.[49]

QUANTIFICATION AND STATISTICAL ANALYSIS

Graphs in the manuscript show mean values. Statistical analyses were performed using GraphPad Prism 8 software (GraphPad Software, Inc.). Unpaired *t* test was used for comparison between two groups, and Tukey's test or Holm–Sidak's test was used for comparison among three or more groups.